On channel gain performance of car roof-glass embedded 5G antenna

Aliakbari Abar, Hanieh; Lötbäck, Christian ; Li, Xiaotian ; Lau, Buon Kiong

Published in:
2025 19th European Conference on Antennas and Propagation (EuCAP)

DOI:
10.23919/EuCAP63536.2025.10999768

2025

Document Version:
Publisher's PDF, also known as Version of record

On Channel Gain Performance of Car Roof-Glass Embedded 5G Antenna

Hanieh Aliakbari[1,2], Christian Lötbäck[1], Xiaotian Li[1], Buon Kiong Lau[2]
[1] Volvo Car Corporation, Gothenburg, Sweden, hanieh.aliakbariabar@volvocars.com
[2] Department of Electrical and Information Technology (EIT), Lund University, Lund, Sweden

***Abstract*— 5G antennas for vehicular connectivity are often mounted on the car roof to optimize signal reception. The trend of replacing metal roof with glass in modern cars opens an opportunity for embedding the 5G antennas inside the glass roof. In this work, we compare the channel gains of reference dipole, and loop antennas positioned at the roof center. Then, by considering the requirements of glass integration and the channel gain performance, a nontransparent wideband monopole antenna with an extended feedline is designed to be embedded inside a real glass roof. To recover the optical transparency of the roof glass while retaining the wideband performance, the metal conductor is replaced with non-uniform metal mesh structure. The proposed semi-transparent wideband monopole antenna covers both 5G and legacy bands. Within the operating frequency range from 617 MHz to 5 GHz, the channel gain and radiation efficiency are above -4.5 dB and 37%, respectively.**

***Index Terms*—automotive antennas, hidden antennas, roof-glass embedded antennas, mean effective gain.**

I. Introduction

Modern cars are equipped with antennas that can receive cellular communication signals [1]. The antennas for cellular communications are often mounted on the car roof to provide minimal radio frequency (RF) signal blockage (see Fig. 1). In recent years, cellular antennas for cars are typically packaged with other antennas in a roof-mounted, protruding antenna module called "shark-fin". However, the sizeable shark-fin structure degrades the car's aesthetic and aerodynamic qualities. To address these challenges and also keep up with the ongoing modern car design trend of replacing the metal roof with glass construction, it was shown that car antenna can be fully embedded inside the glass roof of modern cars [2]. To satisfy the requirements of glass integration, the antenna structure should be planar, low profile, without any lumped component or via through the glass layers.

Cellular systems are currently being upgraded to 5G to provide better services, such as higher throughput and lower latency. However, existing cellular systems including Long Term Evolution (LTE) will continue to be active for many years. Hence, cellular base station and user equipment will need to cover LTE bands (i.e., low bands within 617-960 MHz, mid bands within 1447.9-2170 MHz) together with 5G sub-6 GHz bands (e.g., 2300-5 GHz). To cover the entire frequency range, bandwidth of over 155% is needed, which is difficult to achieve with a single resonant antenna.

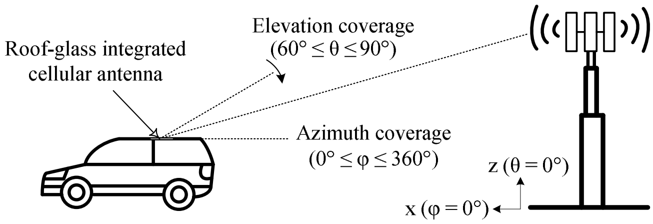

Fig. 1. Elevation and azimuth angles of interest for cellular communication. A cellular antenna can be embedded in the glass roof of the car.

Existing cellular antennas for vehicular applications (e.g., [3]-[8]) cover a wide range of 5G and LTE bands. However, they are not suitable for glass integration and/or do not fully cover the desired band from 617 MHz to 5 GHz. In fact, most of the previous studies on glass-based vehicular antennas deals with low frequency on-glass designs [9]) or higher frequency non-integrated designs [10], [11]. To our knowledge, there is no existing literature on cellular frequency wideband antennas embedded inside the roof-glass. In addition, realistic roof glass and propagation channel are not often considered in existing literature.

In this context, this paper proposes a semi-transparent 5G antenna that is suitable for glass-roof integration and covers the entire frequency range of 617 MHz to 5 GHz. We begin by evaluating the channel gain performance of two reference antennas on the roof of a real car. The effect of the propagation channel is included in the channel gain as defined by mean effective gain (MEG) [12]. Then, by considering the glass integration requirements, a compact wideband 5G antenna is designed by using the multilayer glass as its substrate. To allow for the antenna to be placed in the transparent area of the glass roof, a semi-transparent counterpart is designed, and its performance is evaluated.

II. Simulation Setup

A. Mean Effective Gain

An effective method to predict the overall channel gain of an antenna system in the automotive industry is to calculate the mean effective gain (MEG), which combines the antenna's 3D pattern with the angular power spectrum (APS) of the propagation channel of interest [12]. Since the cellular signals are exchanged with elevated base station antennas, the main directions of arrival of the radio signals at the car roof tend to

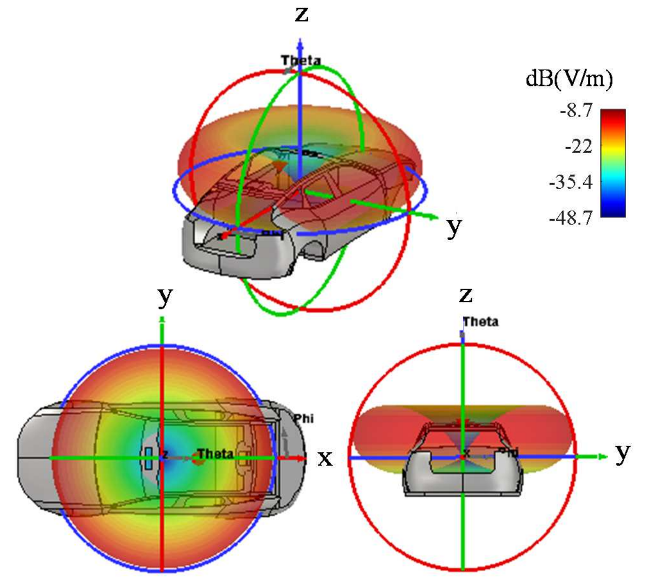

Fig. 2. Different views of the 3D APS superimposed around the intended antenna location on the car roof of a Volvo car model.

be uniformly spread in azimuth (ϕ = [0°, 360°]) but cluster around θ = 60°– 90° in elevation (see Fig. 1). Such a signal distribution can be modeled by a 3D APS with uniform distribution in azimuth and truncated Gaussian distribution in elevation. Figure 2 shows the simulated APS around the intended antenna location on the roof of a Volvo car model, which is used for MEG calculation in this work. The APS in Fig. 2 is uniform distributed in azimuth and Gaussian distributed in elevation with mean of 75° and standard deviation of 15° (i.e., a "raised donut" signal distribution). In the simulations, the APS is assumed to be identical for both polarizations.

In the following subsections, car roof mounted dipole and loop antennas are simulated, and their MEGs and bandwidths are evaluated and used as references for the proposed design.

A. Reference Dipole Antenna

A vertical half-wavelength dipole antenna by itself offers a suitable antenna pattern for cellular communication. This is because its "donut" pattern fits well with the "raised donut" shape of the APS. However, when the dipole antenna is located in the center of the car glass roof, as depicted in Fig. 3(a), the presence of the car body is expected to have an impact on its "donut" pattern. To illustrate the different interactions, we simulated a half-wavelength reference dipole antenna working at a low LTE band (with center frequency of 900 MHz) on the roof location, with either: 1) a roof-only model or 2) a full car model (see Fig. 4 (a)). It is noted that glass windows and roof is removed from either model, to speed up the full-wave simulations, while still capturing the main effects of the car roof/body. The full-wave simulations were performed using the time-domain solver of the 2022 CST Microwave Studio software. The number of mesh cells generated for the roof-only model and the full car model are 26 millions and 425 millions, respectively. As can be seen in

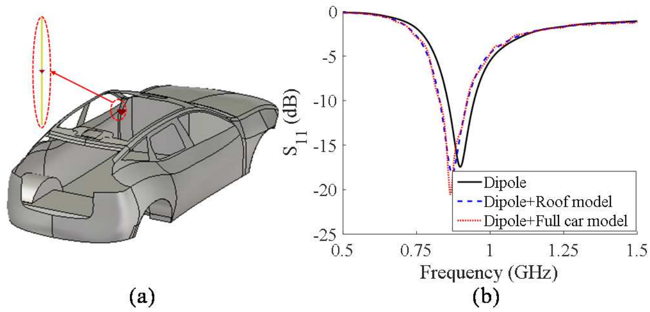

Fig. 3. (a) 3D view and (b) reflection coefficients of the simulated reference dipole and its roof center location on the full car model.

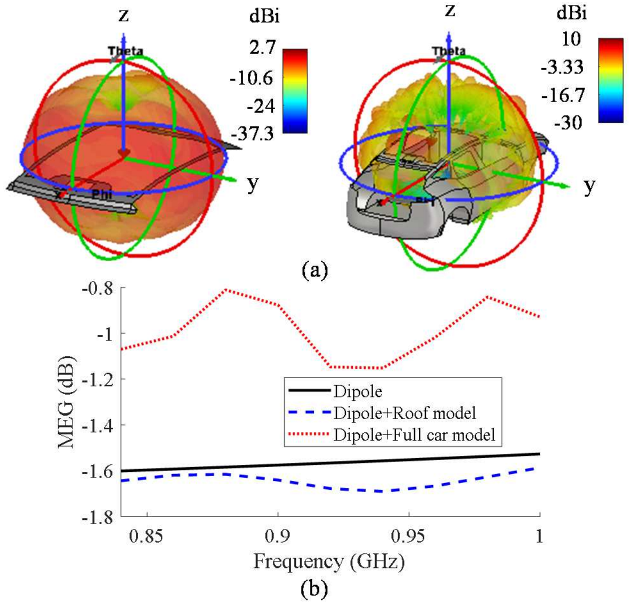

Fig. 4. (a) 3D realized total gain patterens of the reference dipole on the roof and full car model at 900 MHz, (b) MEG of the reference dipole.

Fig. 3(b), the reflection coefficient of the reference dipole is similar for both models, with a small frequency shift (i.e., 20 MHz) compared to the free space (i.e., dipole-only) case for the resonance at 900 MHz. However, the car model interacts with the radiation from the dipole as can be seen in Fig. 4(a), and the MEG has been improved in the case of full car model compared to free space (Fig. 4(b)). The MEGs for the free space and the roof model are similar (i.e., within 0.2 dB) around the resonance due to the roof by itself not being representative of the entire car when it comes to the effect on the radiation pattern. Therefore, to achieve more accuracy, the full car model is used in the subsequent simulations.

Despite of having good MEG, the dipole is not a good candidate for the glass integration, as it has high profile. On the other hand, the gain pattern of a small loop is very similar to a small electric dipole (though offering a different polarization), and it has low profile. So in the next section the performance of the small loop will be evaluated.

A. Reference Loop Antenna

As can be seen in Fig. 5 (a), the reference loop with radius r is now placed in the center location on the roof. The MEGs

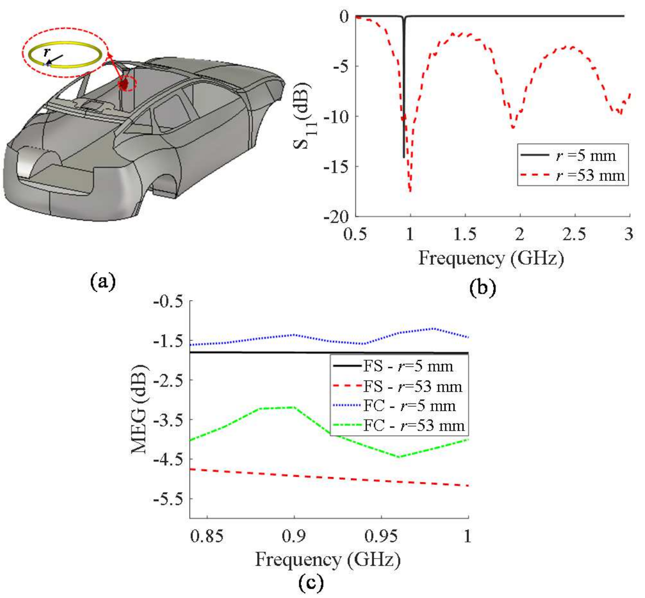

Fig. 5. (a) 3D view of the simulated reference loop with radius r, (b) Reflection coefficients, and (c) MEG of the reference loop monuted on the roof center of the full car model.

of the loop for different cases are shown in Fig. 5(c). It shows good MEG for the case of a small loop in free space (FS) and with full car (FC) model, with $r = 5$ mm. But it was found that as the radius of the reference loop on the roof increases beyond 18 mm, the MEG starts to decrease. For example, the MEG for $r = 53$ mm, as depicted in the figure, show a degradation of around −2 dB or more. The MEG decrease is due to the pattern maximum shifting towards the loop's axis on the car (i.e. upwards). However, the small loop (r =5 mm) needs to be matched with external L-shape LC matching network (i.e., series C = 2.7 pF, parallel L = 18.8 pF) and only offers a narrow band (< 1% at 900 MHz in Fig. 5(b)). However, as the radius is increased to have a circumference of ~1 λ at 900 MHz (i.e., r = 53 mm), the bandwidth will greatly increase (using L-shape matching network, series L = 11.2 nH, C = 1.6 pF), but at the cost of decreased MEG, as discussed. Thus, despite having low profile, loop antenna cannot offer both good MEG and wideband operation.

III. Monopole Antenna

A. Glass Integrated Antenna

As discussed in the Introduction, wideband antennas that can cover all cellular bands are essential for modern cellular wireless communication. Moreover, MEG should also be kept high and stable over the entire band. Furthermore, to facilitate glass integration, the structure should be planar, via-less and of low profile. On the other hand, monopolar antenna pattern is known to be desirable for cellular communications [4], [5]. Monopolar patch antennas can satisfy the propagation channel requirements when it is placed inside the roof-glass. However, it needs a few vias to offer omni-directional pattern, and making vias is extremely challenging for glass integration [13]. Hence, via-less printed monopole antennas, which are good examples of ultra-wideband (UWB) antennas [10], are suitable candidates for integration in the glass.

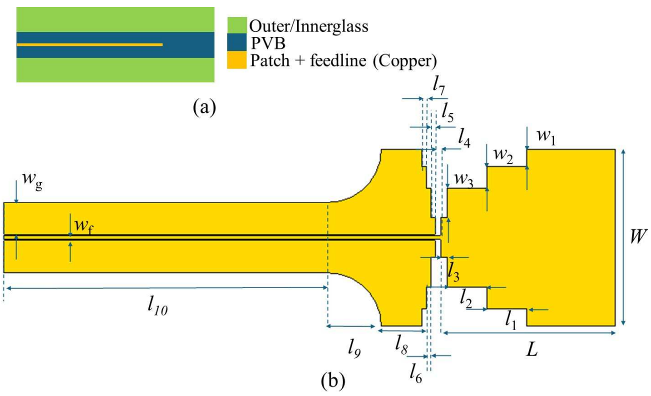

Fig. 6. (a) Cross-section of the proposed glass integrated coplanar waveguide (CPW)-fed printed monopole antenna, and (b) top view with dimensions: W= 82 , L= 81 , l_1= 18.5 , l_2= 18.5 , l_3= 3 , l_4=2.5 , l_5= 2 , l_6= 2 , l_7= 2 , l_8= 18.9 , l_9= 24.6 , l_{10}= 150 , w_1= 8 , w_2= 10 , w_3= 14 , w_g=15 , w_f= 1.8. (Units: mm)

Fig. 6(a) shows the cross-section view of a typical low-profile laminated glass used as the roof glass in real cars. It is composed of an outer glass, an inner glass and a polyvinyl butyral (PVB) layer in-between [14]. As for the antenna topology, a printed monopole with a topology similar to the one considered in [15] is adopted as the radiating element inside the glass. This includes a patch as the main radiating element with the dimensions of $L \times W$, as shown in Fig. 6(b). However, the microstrip feedline [15] is replaced by in-glass coplanar waveguide (CPW) (see Fig. 6 (b)) with the same width as the patch (W). CPW is better for glass integration, since it allows for the antenna and feeding structure to be on the same plane [2]. The width of the antenna's CPW feedline is 1.8 mm to realize a 50 Ω characteristic impedance in the stack up of Fig. 6(a). To avoid sharp discontinuity in the connection point between the feedline and the patch, a few notches are etched at the lower corners. As more bandwidth is required here than the original design [15], three notches with dimensions of $l_i \times w_i$ (i = 1, 2, 3) and three notches with dimensions of $l_i \times w_j$ (i = 5, 6, 7, j = 1, 2, 3) are etched on the patch and CPW ground (GND), respectively. The simulations show that the notches on the CPW's GND mainly improves the impedance matching at lower frequencies.

As depicted in Fig. 6(a), the rectangular patch radiator and the feedline is embedded inside the laminated roof glass. The printed monopole is a via-less design and hence suitable for glass roof implementation. Similarly, to facilitate practical via-less connection to an electronic control unit (ECU), and place the antenna in a general transparent location on the glass, outside of the blackout (i.e., tinted) region, the in-glass CPW feed needs to be extended from the antenna location to one edge of the roof glass [16]. Simulations shows that the width of the in glass CPW GND for the extension line (i.e. w_g) should be smaller than the CPW GND of the radiation element as larger w_g affects the matching. To this end and to avoid discontinuity, the width of the antenna's in-glass CPW line was extended by a smooth transition with the length of l_9 to the input CPW with the width of w_g (see Fig. 6(b)).

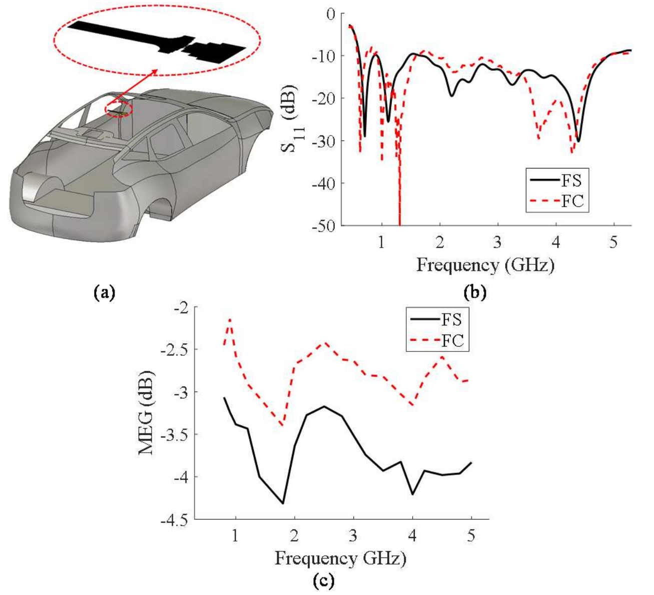

Fig. 7. (a) 3D view of the printed monopole, (b) Reflection coefficients, and (c) MEG of printed monopole monuted on the roof center.

The parameters in Fig. 6(b) were optimized for impedance matching in the cellular bands from 617 MHz to 5 GHz. In this first step, a (nontransparent) copper layer with the thickness of 0.018 mm is used as the conductor. The optimized antenna (with the glass layers but without the extension part, $l_9 + l_{10}$) has the dimensions of $0.2\lambda \times 0.25\lambda \times 0.01\lambda$ at the lowest operating frequency (617 MHz).

B. Simulation Results

The simulated 10 dB impedance bandwidth of the glass-integrated (nontransparent) monopole antenna covers existing cellular bands from 617 MHz to 5 GHz, including sub-6 GHz 5G bands (see Fig. 7(b)). In the simulation model, the roof glass is dimensioned to be rectangular, and it fully covers the antenna and CPW feedline. The MEG is found to be higher than -4.5 dB, with 1.4 dB of variation over the applicable band (see Fig. 7(c)). The relatively low MEG is partly because, unlike the dipole and small loop (whose MEGs are given in Figs. 4(c) and 5(c)), the monopole antenna has a few undesired deep nulls in its pattern in the azimuth, when it is embedded inside the roof glass. On the other hand, the variation in MEG is due to the variation in the radiation pattern over the wide band.

Like the reference dipole and loop antennas in Section II, the monopole antenna's performance was also evaluated in FC simulation (see Fig. 7(a)). The impedance matching of the antenna in the FC setup is almost the same as that of FS case, and the same impedance bandwidth is achieved. The MEG is higher for the FC setup than the FS setup (Fig. 7(c)), with about 1 dB of variation observed within the wide band.

C. Semi-transparent Antenna

To not disturb the functionality of the glass roof, which is transparent, the antenna with high overall optical transparency is more desirable. However, transparent conductors (TCs) are

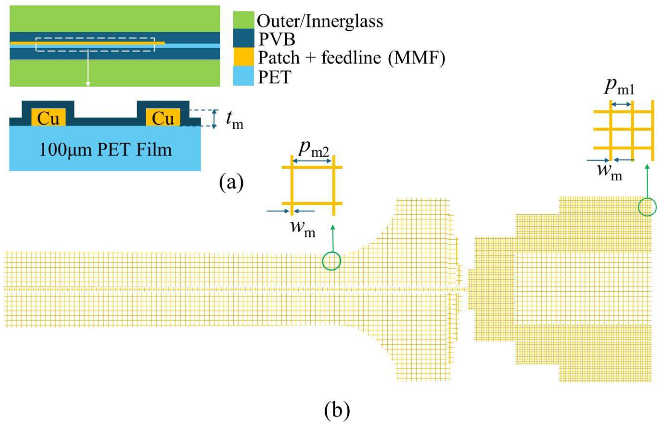

Fig. 8. (a) Cross section of the proposed roof-glass integrated CPW-fed semi-transparent monopole antenna, and (b) top view with a non uniform square-shaped mesh structure with design parameters of (mm), w_m= 0.021, p_{m1}=0.3 , p_{m2}=0.9, t_m=0.005.

typically very lossy at cellular frequencies, which leads to low radiation efficiency of the transparent antennas. In this context, metal mesh film (MMF) presents a good trade-off between the transparency and conductivity [18]. For example, it has been shown that by increasing the pitch (i.e. p_m in Fig. 8 (b)) of the well-known square sheet MMF, the optical transparency (OT) can be increased at the cost of lower conductivity (i.e., higher sheet resistance, R_s) [18]. The copper sheet of the proposed antenna in Fig. 7(b) is replaced by a conductive MMF with a square pattern (see Fig. 8(b)). The MMF only occupies a small portion of the glass surface, and this ensures high transparency of the whole structure. As the strip lines are very thin and fragile, the MMF is placed on a transparent substrate of polyethylene terephthalate (PET), as shown in Fig. 8(a).

A method was proposed for improving the efficiency of antennas made from TC films by applying a highly conductive narrow strip to the edges with high current density [17]. This method is adapted here for the roof glass integrated monopole antenna, using non-uniform MMF as the TC. To identify the regions of high currents, the surface current distribution of the proposed monopole is simulated at different frequencies over the wide operating band. Figure 9 shows that there are lower currents in the inner region of the patch and CPW GND lines, over almost the entire bandwidth. Hence, to have higher transparency for the monopole antenna and consequently the entire glass roof, the MMF with larger pitches (i.e., R_s = 0.15

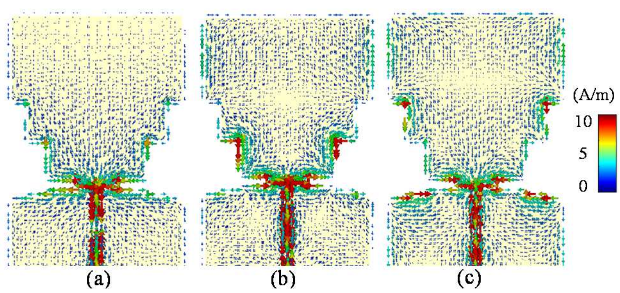

Fig. 9. Surface current of the CPW-fed printed monopole with solid copper at (a) 0.7, (b) 2.1, (c) 4.1 GHz.

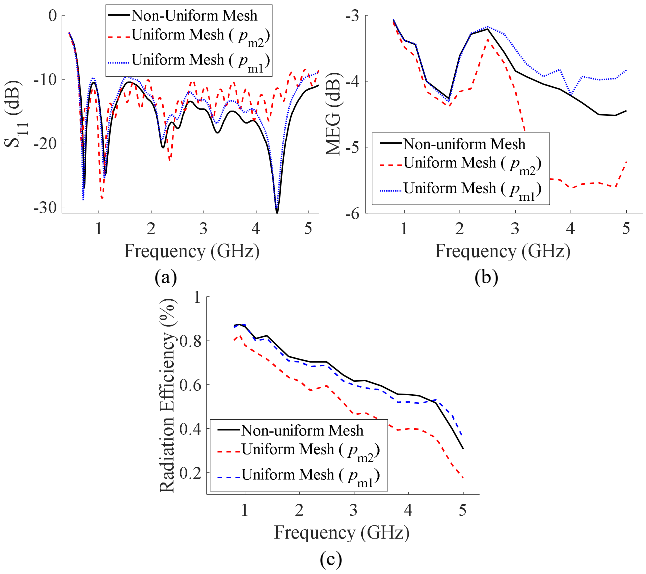

Fig. 10. (a) Reflection coefficient, (b) MEG, and (c) radiation efficiency of printed monopole with uniform and nonuniform MMF in FS.

Ω/sq, OT=95%) has been chosen for the lower current region (see Fig. 8(b)). Moreover, less conductor coverage reduces the usage of the conductive materials which can be expensive and less sustainable. In the higher current regions, the MMF with smaller pitches (i.e., R_s = 0.05 Ω/sq and OT=83%) is used.

It is noteworthy that the performance of the antennas using the uniform MMF with smaller pitch (p_{m1}) is the same as that of the nontransparent counterpart in Fig. 7, which indicates that the difference is negligible for tight meshing. However, using the MMF with larger pitch (p_{m2}) in the regions with higher current density results in worse matching at higher frequencies and more variations over the bandwidth (see Fig. 10(a)). On the other hand, according to the simulated reflection coefficient, we can conclude that the uniform (p_{m1}) and non-uniform transparent monopole antennas have almost the same results in the targeted band with slightly broader operating bandwidth for the latter. Figure 10(b) shows that the MEG has about 2.6 dB variation over the band for uniform larger mesh (p_{m2}), which is ~1 dB more than that of the non-uniform MMF. The radiation efficiencies for the non-uniform and uniform mesh structures are shown in Fig. 10(c). In the case of non-uniform mesh, the efficiency is more than 37% over the operating band, while it is higher than 19% over the band for uniform mesh (p_{m2}). This is mainly due to the higher sheet resistance for the uniform mesh and the more restrictive current distribution relative to the nonuniform counterpart.

IV. Conclusion

In this paper, the channel gain performance of different antennas on the car roof have been evaluated. It has been demonstrated that a single layer printed monopole antenna can be tuned to cover 155% bandwidth upon integration into a car's roof glass. Feeding via an extended CPW feed allows for the antenna to be freely positioned on the roof and avoids the need to drill vias through the glass layers. Creating non-uniform mesh structure allows the antenna to maintain good MEG and transparency for reduced conductor usage, leading to lower fabrication cost and better sustainability.

References

[1] I. M. Yousaf, H. Aliakbari, and B. K. Lau, "Quad-element LTE hidden car roof antenna system," *IEEE Antennas Wireless Propag. Lett.*, vol. 22, no. 11, pp. 2755-2759, Sep. 2023.

[2] H. Aliakbari, X. Li, C. Lötbäck, and B. K. Lau, "Roof-glass integrated antenna for vehicular GNSS applications," *in Proc. 18th Europ. Conf. Antennas Propag. (EUCAP'2024)*, Glascow, Scotland, Mar. 2024.

[3] S. Hastürkoğlu and S. Lindenmeier, "A wideband automotive antenna for actual and future mobile communication 5G/LTE/WLAN with low profile," in *Proc. Eur. Conf. Antennas Propag. (EUCAP'2017)*, Paris, France, Mar. 2017.

[4] M. O. Khalifa, A. M. Yacoub, and D. N. Aloi, "A multiwideband compact antenna design for vehicular sub-6 GHz 5G wireless systems," *IEEE Trans. Antennas Propag.,* vol. 69, no. 12, pp. 8136-8142, Dec. 2021.

[5] H. Lee, H. J. Song, and N. Eshaq, "Compact UWB cellular antenna integrated into vehicle spoiler," in *Proc. IEEE Antennas Propag. Soc. Int. Symp. (APS'2022)*, Denver, CO, USA, Jul. 2022.

[6] D. Navarro, *et al.*, "Compact wideband Vivaldi monopole for LTE mobile communications," in *Proc. IEEE Antennas Propag. Soc. Int. Symp. (APS'2013)*, Orlando, FL, USA, Jul. 2013.

[7] A. Yacoub, M. Khalifa, and N. D. Aloi, "Wide bandwidth low profile PIFA antenna for vehicular sub-6 GHz 5G and V2X wireless systems," *Prog. Electromagn. Res. C*, vol. 109, pp. 257-273, 2021.

[8] A. Michel, *et al*., "Printed wideband antenna for LTE-band automotive applications," *IEEE Antennas Wireless Propag. Lett.*, vol. 16, pp. 1245-1248, Nov. 2017.

[9] S. Ahn and H. Choo, "A systematic design method of on-glass antennas using mesh-grid structures," *IEEE Trans. Veh. Technol.*, vol. 59, no. 7, pp. 3286–3293, Sep. 2010.

[10] B. T. P. Madhav, T. Anilkumar, and S. K. Kotamraju, ''Transparent and conformal wheel-shaped fractal antenna for vehicular communication applications,'' *AEU-Int. J. Electron. Commun*., vol. 91, pp. 1-10, Jul. 2018.

[11] D. Potti, G. N. A. Mohammed, K. Savarimuthu, and B. B. Pamula, "Multilayer thin film based optically transparent dual-band automotive windshield antenna," *Int. J. RF Microw. Comput.-Aided Eng*., vol. 32, no. 4, Apr. 2022.

[12] T. Taga, "Analysis for mean effective gain of mobile antennas in land mobile radio environments," *IEEE Trans. Veh. Technol*., vol. vol. 39, no. 2, pp. 117-131, May 1990.

[13] H. Wong, K. K. So, and X. Gao, "Bandwidth enhancement of a monopolar patch antenna with V-shaped slot for car-to-car and WLAN communications," *IEEE Trans. Veh. Technol*., vol. 65, no. 3, pp. 1130-1136, Mar. 2016

[14] Sekisui Chemical Co. Ltd., "What is PVB interlayer?" www.s-lecfilm.com. https://www.s-lecfilm.com/en/PVB-interlayer/ (assessed Oct. 9, 2023).

[15] J. Jung, W. Choi, and J. Choi, "A small wideband microstrip-fed monopole antenna," *IEEE Microw, Wireless Compon. Lett.*, vol. 15, no. 10, pp. 703-705, Oct. 2005.

[16] H. Aliakbari, X. Li, C. Lötbäck, and B. K. Lau, "Effect of coplanar waveguide feedline on car roof-glass integrated GNSS antenna performance," in *Proc. IEEE Antennas Propag. Soc. Int. Symp. (APS'2024)*, Firenze, Italy, Jul. 2024.

[17] H. J. Song, *et al.*, "A method for improving the efficiency of transparent film antennas," *IEEE Antennas Wireless Propag. Lett.,* vol. 7, pp. 753-756, 2008.

[18] P. D. Tung and C. W. Jung, "Optically transparent wideband dipole and patch external antennas using metal mesh for UHD TV applications," *IEEE Trans. Antennas Propag*., vol. 68, no. 3, pp. 1907-1917, Mar. 2020.